CARBON 71 (2014) 87–93

Available at www.sciencedirect.com

ScienceDirect

journal homepage: www.elsevier.com/locate/carbon

Photoluminescent carbon dots directly derived from polyethylene glycol and their application for cellular imaging

Rui-Jun Fan [a], Qiang Sun [a], Ling Zhang [a], Yan Zhang [b,*], An-Hui Lu [a,*]

[a] State Key Laboratory of Fine Chemicals, School of Chemical Engineering, Dalian University of Technology, Dalian 116024, PR China
[b] Dalian Medical University affiliated No. 1 Hospital, Dalian 116021, PR China

ARTICLE INFO

Article history:
Received 24 December 2013
Accepted 13 January 2014
Available online 16 January 2014

ABSTRACT

Photoluminescent carbon dots (C-dots) were prepared directly by a simple hydrothermal treatment using polyethylene glycol with different molar weight (400–6000 g mol^{-1}) as the sole carbon source. The synthesized C-dots with tunable diameters of 2–4 nm exhibit excitation-dependent photoluminescent behavior. In contrast to previous methods, neither strong acid treatment nor further surface modification is necessary for this one-step process. The C-dots with well-defined surface chemistry and properties were well-dispersed in aqueous media and showed high photostability indicating they are suitable for use in different pH and NaCl aqueous solutions. The C-dots possessed low cytotoxicity, good photostability and can enter the cancer cells, making them suitable candidates for two-photon cellular imaging and labelling.

1. Introduction

Fluorescent nanoparticles have been paid more and more attention due to their abundant optical properties and their myriad applications in biology, chemistry and so on [1–3]. To date, typical photoluminescent particles have been developed from compounds of lead, cadmium, gold, silver and silicon [4–7]. But these materials also have raised concerns over potential toxicity, environmental harm and highly valued [8,7]. Therefore, it is very desirable to develop a simple, inexpensive method for the synthesis of highly fluorescent nanoparticles with good photostability and low toxicity.

In recent years, carbon dots (C-dots) have attracted great interest due to their low cost, versatile surface chemistry, stable photoluminescent (PL) properties, and good biocompatibility [9–12]. Top-down approaches, including laser ablation [13–15], electrochemical oxidation [16], confined combustion [17], and chemical oxidation using nitric acid [18–20] are currently regarded as state-of-the-art methods to synthesize C-dots. However, these processes involving complex and extreme synthesis conditions, are time- and energy-consuming, and require expensive reagents or apparatus. Furthermore, bottom-up approaches such as the carbonization of chemical precursors (e.g., glucose, sucrose, glycol, glycerol, citric acids and L-ascorbic acid, etc.) [21–26] have received significant attention for the production of fluorescent C-dots. Typically, these C-dots require further surface oxidation and/or passivation to render them fluoresce and simultaneously hydrophilic surface [27]. Thus, it is a very challenging goal to develop a simple method for the synthesis of self-passivated C-dots.

It's been recognized that polyethylene glycol (PEG) can be used as a passivating agent or solvent to fabricate biocompatible C-dots having bright and excitation-tunable photoluminescence, as it is non-toxic and non-immunogenic and easily conjugated to other biomolecules using simple chemistry methods [13,28–31]. For example, PEG-1500 N was used as a surface passivation agent to synthesize PEG-1500-passivated C-dots [30]. Du et al. have reported an effective method for the synthesis of fluorescent C-dots by laser irradiation of a

* *Corresponding authors:* Fax: +86 411 84986112 (A.-H. Lu).
E-mail addresses: zhangyanmed@126.com (Y. Zhang), anhuilu@dlut.edu.cn (A.-H. Lu).
0008-6223/$ - see front matter
http://dx.doi.org/10.1016/j.carbon.2014.01.016

carbon suspension in an organic solvent [32]. Synthesis and surface modification of the C-dots were believed to occur simultaneously. Yang et al., have presented an easy, economical microwave pyrolysis approach to synthesize fluorescent carbon nanoparticles using saccharide as the carbon precursor and PEG-200 as passivating agent [33]. More recently, Jaiswal et al. have reported a simple microwave mediated method for synthesizing C-dots using PEG as both carbon precursor and passivating agent [34]. Irradiation of the aqueous PEG-200 solution by microwaves in a 900 W domestic microwave oven for 10 min resulted in the formation of C-dots. However, experiments with polymers with a molecular weight higher than 600 did not yield any discernable C-dots.

Here, we have established a one-step hydrothermal route to prepare fluorescent C-dots from non-conjugated polymers PEG (400–6000 g mol^{-1}) without further surface modification. Compared with the previous works using PEG to prepare C-dots, our devised method does not need additives (acid, base and/or salt), organic solvent, and further surface passivation. Moreover, the synthesis was conducted at mild reaction conditions. Remarkably, the as-synthesized C-dots with defined surface chemistry and properties can be dispersed well and show excitation tunable luminescence, high photostability and are suitable for use in different pH and NaCl aqueous solutions. Coupled with the characteristic PL properties and enhanced colloidal stability in salt conditions, the as-synthesized C-dots are promising candidates for cellular imaging. Besides, this one-step preparation process of C-dots from the mixture is simple and effective, and has potential for large-scale production.

2. Experimental

2.1. Synthesis of C-dots

PEGs with different molecular weights (PEG-400, PEG-1500 and PEG-6000) were purchased from the Sinopharm Chemical Reagent Co., Ltd. and used without further purification.

The PEG (3 g) was dissolved in deionized water (10 mL) in a glass beaker. The solution was transferred into a 50 mL Teflon-lined stainless steel autoclave and heated at 120 °C for 72 h and then cooled to room temperature naturally. Subsequently, the aqueous solution was subjected to dialysis (3 days, changing the deionized water every 4 h). Finally, a yellow aqueous solution containing C-dots was obtained and named C-*n* (where *n* indicates the molar weight of the PEG).

2.2. Characterization

Transmission electron microscopy (TEM) analyses were carried out using a Tecnai $G^2$20S-Twin instrument operating at 200 kV. The samples for TEM analysis were prepared by dropping an ethanol droplet of the products onto carbon-coated copper grids and drying at room temperature. Fluorescence spectroscopy was performed with a Hitachi F-7000 spectrophotometer at different excitation wavelengths ranging from 325 to 500 nm. UV–vis absorption spectra were obtained using a TECHCOMP UV–vis 2300 spectrophotometer. Fourier transform infrared spectroscopy (FTIR) spectra were measured with a Thermo Nicolet 6700 spectrometer ranging from 650 to 4000 cm^{-1}. Time-resolved fluorescence intensity decay of the C-dots was recorded using a FL900 spectrofluorimeter (Edinburgh Instrument). The sample was excited by a 405 nm laser, and the signal was monitored at 480 nm. Fluorescence imaging studies were performed with an Olympus FV1000 inverted fluorescence microscope, where the cells were excited with 800 nm two-photon laser pulses.

2.3. Quantum yield measurements

The quantum yield of the C-dots was calculated using following equation:

$$\Phi = \Phi_R \times \frac{I}{I_R} \times \frac{A_R}{A} \times \frac{\eta^2}{\eta_R^2}$$

The quinine sulfate ($\Phi_R = 0.54$) was dissolved in 0.1 M H_2SO_4 (refractive index (η) of 1.33) and C-dots were dissolved in deionized water ($\eta = 1.33$). Where, Φ and I are the quantum yield and integrated emission intensity, η and A are the refractive index and optical density. The subscript R refers to the reference fluorophore of known quantum yield. In order to minimize re-absorption effects, absorbance in the 1 cm quartz cuvette was kept below 0.10 at an excitation wavelength of 360 nm.

2.4. Cytotoxicity experiment

The in vitro cytotoxicity was assessed using the 3-[4,5-dimethylthiazol-2-yl]-2,5-diphenyltetrazolium bromide (MTT) assay in Hep G2 cells. Initially, cells were seeded into a 24-well cell-culture plate (Corning™) at $\sim 4 \times 10^4$ per well in a RPMI 1640 medium supplemented with 10% newborn calf serum (NCS) and 1% penicillin–streptomycin solution. After incubation for 20 h at 37 °C under 5% CO_2, RPMI 1640 solutions of C-400 (1 mL per well) with several concentrations (0, 50, 100, 200 and 400 mg mL^{-1}) were added to each well. The cells were further incubated for 24 h at 37 °C under 5% CO_2. Subsequently, 1 mL RPMI 1640 and 0.1 mL MTT (5 mg mL^{-1} in PBS solution) were added to each well. Following incubation for an additional 4 h, the medium was removed and 0.75 mL dimethyl sulfoxide (DMSO) was added to each well. After 15 min, the solution of each well was centrifuged, and then supernatants were transferred to a 96-well plate. Finally, the optical density (OD) at 570 nm of each well was measured on a Synergy H1 Hybrid multi-mode microplate reader. The cell viability was assessed by the ratio of OD values from each group and control group.

2.5. Cellular imaging

MCF-7 cells (human breast cancer) were maintained in Dulbecco's modified Eagle medium (DMEM) supplemented with 10% fetal bovine serum, 100 units/mL penicillin and 100 mg/mL streptomycin. The cells were incubated at 37 °C in 5% CO_2. Two days before imaging, cells were plated on tissue culture plates, and then incubated in fresh media at 37 °C, 5% CO_2. The cells were then incubated with the C-dots in the DMEM medium for 3 h, and the medium was removed

and the cells washed with PBS 3 times. Finally, 1 mL of PBS was added to the plate and the cells were observed under inverted fluorescence microscopy.

3. Results and discussion

3.1. The synthesis and characterization of C-dots

PEG, as a biocompatible non-conjugated polymer, was used as both carbon source and passivating agent to synthesize carbon dots. The PEG solution itself is a colorless and transparent liquid and non-emissive in the visible region under UV light. After hydrothermal reaction, the solution changed from colorless to yellow, where the present C-dots freely disperse in water with transparent appearance without further ultrasonic dispersion. The pH value of the fresh C-dots was *ca.* 3 because of the formation of carboxyl groups. Herein, PEG-400, PEG-1500 and PEG-6000 were used as the sole carbon source to fabricate C-dots. Typical products synthesized using PEG-400, 1500 and 6000 have been accordingly named C-400, C-1500 and C-6000.

As shown in Fig. 1, the three samples consist of well-dispersed nanoparticles with very narrow size distributions. According to TEM observation (Fig. 1), the statistical particle size distributions of C-400, C-1500 and C-6000 are mainly in the range of 2–4 nm and have average diameters of 3.0, 3.3 and 3.5 nm, respectively (over 100 random nanoparticles were measured per sample). Results show that, C-dots derived from PEG with larger molecular weight give a slightly larger particle size and a relatively wider size distribution. Although three PEG with different molecular weight have been used for the synthesis of carbon dots, the obtained products show almost identical morphology. The major formation path of the C-dots is the dehydration and carbonization mechanism during hydrothermal synthesis. In addition, lots of peroxyl radicals ($HOO^{\cdot}$) can be generated during a hydrothermal process, which can react with the carbon chain of the PEG [9,10,36].

Fig. 2a shows the absorption and emission spectra of the as prepared C-400. The absorption spectrum shows an edge at *ca.* 330 nm and a peak at 256 nm which is ascribed to the π–π^* transition of nanocarbons [35,36]. The PL spectrum shows

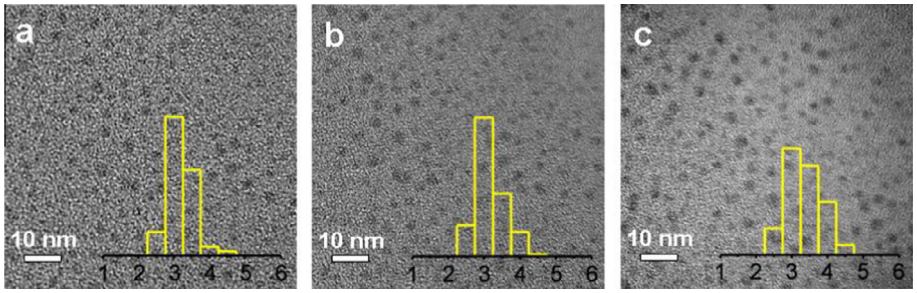

Fig. 1 – TEM images of C-400 (a), C-1500 (b) and C-6000 (c). The overlays are the corresponding particle size distribution histograms. (A color version of this figure can be viewed online.)

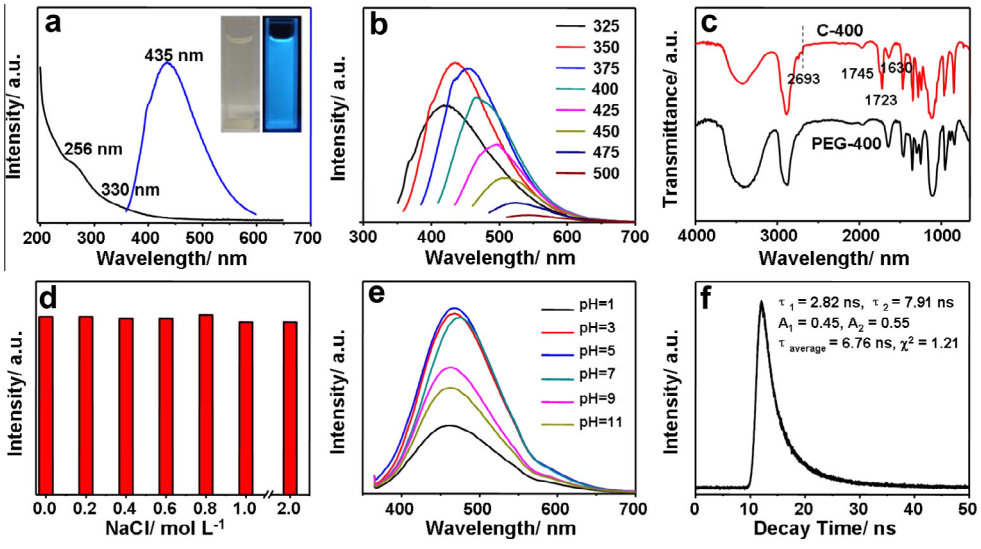

Fig. 2 – (a) UV absorption and PL emission spectra (λ_{ex} = 360 nm) of C-400, Inset: optical images under daylight (left) and UV light (right). (b) Emission spectra of C-400 recorded for progressively longer excitation wavelengths with 25 nm increments from 325 to 500 nm. (c) FTIR spectra of PEG-400 and C-400. Fluorescence intensity of sample C-400 in (d) NaCl solutions with pH = 3, and (e) a solution with different pH. (f) The fluorescence decay profile and the parameter generated by the exponential fitting (inset) (λ_{ex} = 405 nm and λ_{em} = 480 nm) of C-400 aqueous solution. (A color version of this figure can be viewed online.)

Table 1 – Quantum yield of the C-dots samples.

Substance	Area	Abs. at 360 nm	Refractive index	QY (%)
Quinine sulfate	236930	0.100	1.33	54
C-400	8181	0.054	1.33	3.5
C-1500	5394	0.049	1.33	2.5
C-6000	5304	0.052	1.33	2.3

an optimal emission peak at 435 nm when excited at 360 nm (Fig. 2a). The full width at half maximum (FWHM) is *ca.* 100 nm, which is approximately equal to that of most reported C-dots [37,38]. The inset in Fig. 2a shows the optical images of the C-dots under the illumination of sunlight and UV light (365 nm, center), respectively. The bright blue PL of the C-dots is strong enough to be easily seen with the naked eyes. Using quinine sulfate as a reference, a PL quantum yield (QY) of 3.5% was measured (Table 1). The strong fluorescence exhibited by the C-dots may be attributed to the quantum confinement of the passivated surface energy traps [13]. As seen in Fig. 2b, with an increase in the excitation wavelength from 325 to 500 nm, the emission from C-400 gradually shifts to higher wavelengths accompanied by a decreased fluorescence intensity. This is mainly attributed to the different particle size and a considerable distribution of emissive trap sites on each C-dot [13,33].

To gain further insight into the structure of the C-dots, FTIR spectra were acquired to determine the surface properties of samples C-400 and PEG-400; the results are shown in Fig. 2c. Compared with PEG-400, the FTIR spectrum of C-400 shows a new band at 1723 cm^{-1} corresponding to the stretching vibration of C=O, whereas the bands at *ca.* 1745 and 1060 cm^{-1} are ascribed to the carboxylic groups. The bands at *ca.* 2963 and 1630 cm^{-1} correspond to the C=C stretching modes of polycyclic aromatic hydrocarbons. It is clear that the surfaces of the C-dots were partially oxidized, and hydroxy groups were transformed to carboxylate groups. However, surface hydrophilic groups could stabilize the C-dots in aqueous solution and provide the means of hydrophilic reactions. Meanwhile, the carbonization of PEG occurred during the hydrothermal treatment. The bands appearing at 800–900 cm^{-1} correspond to aromatic C–H bond vibrations [14,39,40].

The as-obtained C-dots possess excellent solubility in water without any further surface passivation, which may originate from the –OH groups of the PEG. The fluorescent property of the C-400 at different ionic strengths was monitored while increasing the concentration of NaCl solution from 0 to 2.0 M. As shown in Fig. 2d, there were no changes in either the PL intensities or the peak characteristics, which is of benefit for the use of C-dots in NaCl solutions. The stability of the C-dots in high-salt conditions ensures their applications in more complicated and harsh conditions. Another interesting phenomenon is the pH-dependent PL behavior that PL intensities decrease in solutions with higher or lower pH than *ca.* 5 and C-400 giving the highest PL intensity (Fig. 2e). Fluorescence lifetime is the characteristic period that the C-dot remains in its excited state prior to returning to its ground state. Typically measured in nanoseconds, fluorescent lifetime is an intrinsic property of C-dots that depends on the nature of the fluorescent sites and the environment. The fluorescence lifetime (τ) of C-dots was assessed by time-resolved photoluminescence measurements. As seen in Fig. 2f, the decay trace was fitted using biexponential functions Y(t) based on a non-linear least squares analysis using the following equation: $Y(t)=A_1\exp(-t/\tau_1)+A_2\exp(-t/\tau_2)$, where A_1 and A_2 are the fractional contributions of time-resolved decay lifetime of τ_1 and τ_2. The biexponential behavior of the lifetime suggests that two different emissive sites are present. This implies the fluorescence state is due to the graphite center (or conjugated structures) and surface traps. Further, we calculated the average lifetime ($\tau_{average}$) of C-400 using $\tau_{average} = (A_1\tau_1^2 + A_2\tau_2^2)/(A_1\tau_1 + A_2\tau_2)$, as 6.76 ns ($\chi^2 < 1.21$), which is comparable to other reported values [9,32].

The UV absorption and PL emission spectra of C-1500 and C-6000 were also studied, and found to be similar to those of C-400 (Fig. 3). The PL spectra in Fig. 3a and c show optimal emission peaks at 453 and 445 nm when excited at 360 nm. This is due to the fact that the PL behavior also depends on the synthesis process, such as the passivation conditions and carbon source. We also calculated the QY of C-1500 and C-6000 as 2.5% and 2.3% respectively (Table 1). In addition, the two C-dots (C-1500 and C-6000) also exhibited excitation-dependent PL behavior. As they were excited at wavelengths from 325 to 500 nm, the PL peak shifted from 450 to 550 nm and the PL intensity decreased remarkably (Fig. 3b and e). Such excitation-dependent PL behavior makes the as-prepared C-dots appropriate candidates for extensive applications such as bioimaging, biolabeling and development of optoelectronic devices. Moreover, we also measured the fluorescence lifetime (τ) of sample C-1500 and C-6000. As seen in Fig. 3c and f, the decay traces were both fitted biexponential function, which also indicated two different emissive sites.

3.2. *Two-photon cellular imaging of C-dots*

Two-photon fluorescence imaging with advantages such as a larger penetration depth, minimized tissue autofluorescence background, and reduced photo damage in biotissues has received much attention for its promising applications in both basic biological research and clinical diagnostics [41,42]. As a 'proof-of-concept', we carried out an in vitro two-photon bioimaging study of C-400 using human breast cancer cell lines (MCF-7) by a fluorescence microscope. After incubation with the C-400 at 37 °C for 3 h, the MCF-7 cells under living conditions became brightly illuminated when imaged under the microscope with excitation at 800 nm. The obtained images clearly visualize the bright field image of MCF-7 cells

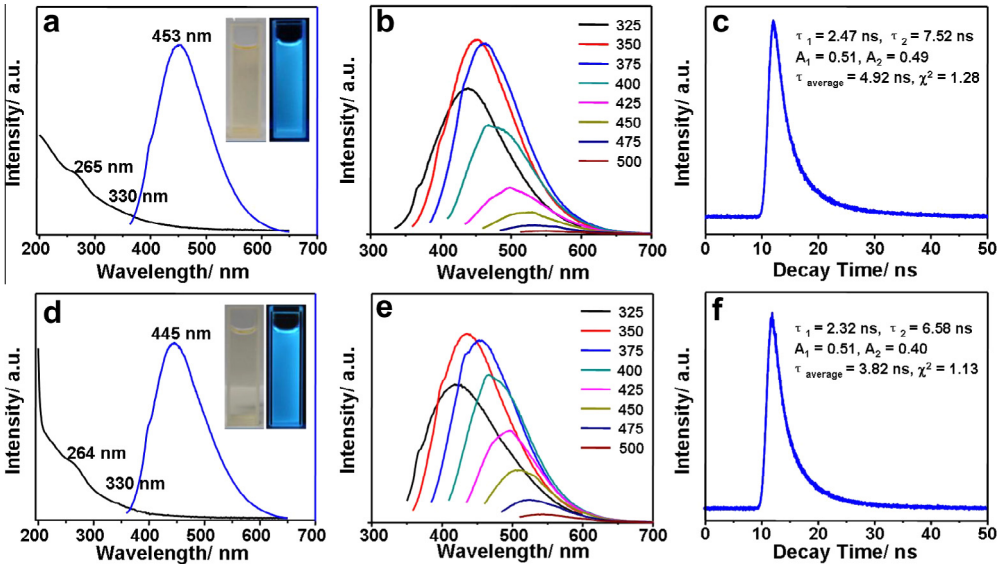

Fig. 3 – UV absorption and PL emission spectra (λ_{ex} = 360 nm) of (a) C-1500 and (d) C-6000, Inset: optical images under daylight (left) and UV light (right). Emission spectra of (b) C-1500 and (e) C-6000 recorded for progressively longer excitation wavelengths with 25 nm increments from 325 to 500 nm. The fluorescence decay profile and the parameter generated by the exponential fitting (inset) (λ_{ex} = 405 nm and λ_{em} = 480 nm) of (c) C-1500 and (f) C-6000 aqueous solution. (A color version of this figure can be viewed online.)

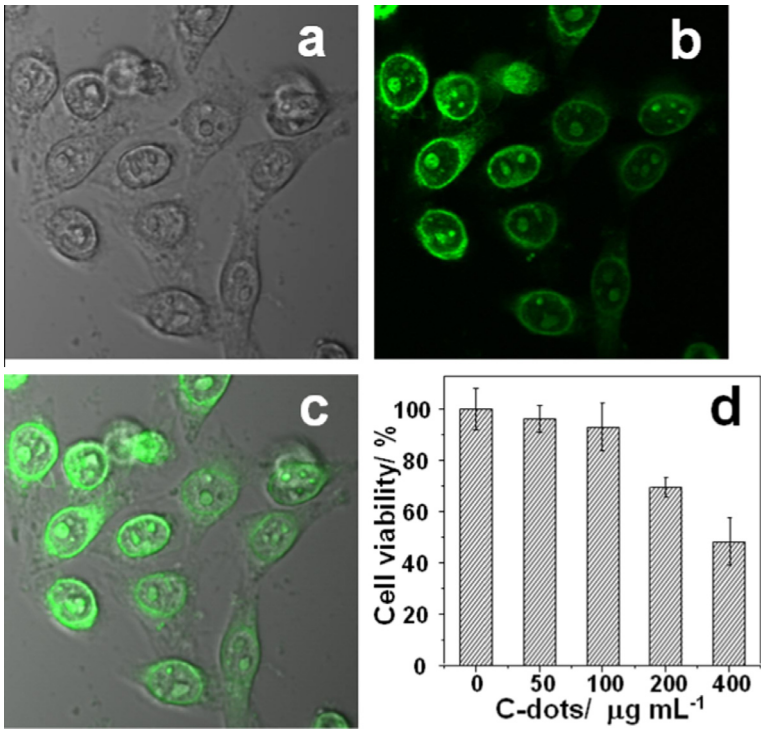

Fig. 4 – Two-photo cellular imaging under (a) bright field and (b) 800 nm excitation. (c) The merged image of a and b. (d) Cell viability of Hep G2 cells after 24 h treatment with C-400 calculated from MTT assay. (A color version of this figure can be viewed online.)

(Fig. 4a), high contrast fluorescence image of C-400 distributed around cytoplasm (Fig. 4b), and the merged image of cell with the bright field and the green fluorescence images (Fig. 4c), displaying that the C-dots can label both the cell membrane and the nucleus of MCF-7 cells. Besides the strong two-photon fluorescence and good stability in the physiological conditions, the C-dots also show quite low cytotoxicity as shown in Fig. 4d. Evaluation of in vitro toxicity of the C-400 was conducted using Hep G2 cells as representative cell lines. It was found that more than 90% of the cells

were viable when incubated with 100 μg mL^{-1} or lesser C-dots. Moreover, nearly 49% of the cells were viable even at a concentration of 400 μg mL^{-1}. The efficient cellular uptake, nontoxicity, and strong two-photon fluorescence show that the obtained C-dots can be used as excellent two-photon probes for high contrast bioimaging.

4. Summary

We have developed a simple method for the one-step hydrothermal synthesis of PL C-dots with small size of 2–4 nm. The dots are directly fabricated derived from PEG with different molar weight (400 to 6000 g mol^{-1}), a biocompatible non-conjugated polymer, as the sole source of carbon and passivating agent. The as-synthesized C-dots have well-defined surface chemistry and properties. They were dispersible in water and showed excitation tunable luminescence, high photostability and are suitable for use in different pH and NaCl aqueous solutions. They also possessed excellent biocompatibility and low toxicity, and can be used as excellent two-photon probes for high contrast bioimaging. Coupled with the characteristic PL properties and enhanced colloidal stability of the C-dots, they are promising candidates for biological and biomedical applications.

Acknowledgments

The project was supported by National Science Fund for Distinguished Young Scholars (No. 21225312) and Special Program for Basic Research of the Ministry of Science and Technology (No. 2012CB626802).

REFERENCES

[1] Michalet X, Pinaud FF, Bentolila LA, Tsay JM, Doose S, Li JJ, et al. Quantum dots for live cells, in vivo imaging, and diagnostics. Science 2005;307:538–44.
[2] Gao XH, Cui YY, Levenson RM, Chung LWK, Nie SM. In vivo cancer targeting and imaging with semiconductor quantum dots. Nat Biotechnol 2004;22:969–76.
[3] Medintz IL, Uyeda HT, Goldman ER, Mattoussi H. Quantum dot bioconjugates for imaging, labeling and sensing. Nat Mater 2005;4:435–46.
[4] Su YY, He Y, Lu HT, Sai LM, Li QN, Li WX, et al. The cytotoxicity of cadmium based, aqueous phase-synthesized, quantum dots and its modulation by surface coating. Biomaterials 2009;30:19–25.
[5] Reiss P, Protière M, Li L. Core/shell semiconductor nanocrystals. Small 2009;5(2):154–68.
[6] Kang ZH, Liu Y, Tsang CHA, Ma DDD, Fan X, Wong NB, et al. Water-soluble silicon quantum dots with wavelength-tunable photoluminescence. Adv Mater 2009;21(6):661–4.
[7] Chan WCW, Nie SM. Quantum dot bioconjugates for ultrasensitive nonisotopic detection. Science 1998;281:2016–8.
[8] Hardman R. A toxicologic review of quantum dots: toxicity depends on physicochemical and environmental factors. Environ Health Perspect 2006;114(2):165–72.
[9] Baker SN, Baker AJ. Luminescent carbon nanodots: emergent nanolights. Angew Chem Int Ed 2010;49(38):6726–44.
[10] Li H, Kang Z, Liu Y, Lee ST. Carbon nanodots: synthesis, properties and applications. J Mater Chem 2012;22(46):24230–53.
[11] Lu AH, Hao GP, Sun Q, Zhang XQ, Li WC. Chemical synthesis of carbon materials with intriguing nanostructure and morphology. Macromol Chem Phys 2012;213(10–11):1107–31.
[12] Qiao ZA, Huo Q, Chi M, Veith GM, Binder AJ, Dai S. A "ship-in-a-bottle" approach to synthesis of polymer dots@silica or polymer dots@carbon core-shell nanospheres. Adv Mater 2012;24(45):6017–21.
[13] Sun YP, Zhou B, Lin Y, Wang W, Fernando KAS, Pathak P, et al. Quantum-sized carbon dots for bright and colorful photoluminescence. J Am Chem Soc 2006;128(24):7756–7.
[14] Wang J, Wang CF, Chen S. Amphiphilic egg-derived carbon dots: rapid plasma fabrication, pyrolysis process, and multicolor printing patterns. Angew Chem Int Ed 2012;51(37):9297–301.
[15] Hu SL, Niu KY, Sun J, Yang J, Zhao NQ, Du XW. One-step synthesis of fluorescent carbon nanoparticles by laser irradiation. J Mater Chem 2009;19(4):484–8.
[16] Zhao QL, Zhang ZL, Huang BH, Peng J, Zhang M, Pang DW. Facile preparation of low cytotoxicity fluorescent carbon nanocrystals by electrooxidation of graphite. Chem Commun 2008;41:5116–8.
[17] Rahy A, Zhou C, Zheng J, Park SY, Kim MJ, Jang I, et al. Photoluminescent carbon nanoparticles produced by confined combustion of aromatic compounds. Carbon 2012;50(3):1298–302.
[18] Tian L, Ghosh D, Chen W, Pradhan S, Chang X, Chen SW. Nanosized carbon particles from natural gas soot. Chem Mater 2009;21(13):2803–9.
[19] Liu HP, Ye T, Mao CD. Fluorescent carbon nanoparticles derived from candle soot. Angew Chem Int Ed 2007;46(34):6473–5.
[20] Krysmann MJ, Kelarakis A, Giannelis EP. Photoluminescent carbogenic nanoparticles directly derived from crude biomass. Green Chem 2012;14(11):3141–5.
[21] Zhang B, Liu CY, Liu Y. A novel one-step approach to synthesize fluorescent carbon nanoparticles. Eur J Inorg Chem 2010;28:4411–4.
[22] Sahu S, Behera B, Maiti TK, Mohapatra S. Simple one-step synthesis of highly luminescent carbon dots from orange juice: application as excellent bio-imaging agents. Chem Commun 2012;48(70):8835–7.
[23] Ma Z, Ming H, Huang H, Liu Y, Kang Z. One-step ultrasonic synthesis of fluorescent N-doped carbon dots from glucose and their visible-light sensitive photocatalytic ability. New J Chem 2012;36(4):861–4.
[24] Jiang J, He Y, Li S, Cui H. Amino acids as the source for producing carbon nanodots: microwave assisted one-step synthesis, intrinsic photoluminescence property and intense chemiluminescence enhancement. Chem Commun 2012;48:9634–6.
[25] Li H, He X, Liu Y, Huang H, Lian S, Lee ST, et al. One-step ultrasonic synthesis of water-soluble carbon nanoparticles with excellent photoluminescent properties. Carbon 2011;49:605–9.
[26] Bourlinos AB, Karakassides MA, Kouloumpis A, Gournis D, Bakandritsos A, Papagiannouli I, et al. Synthesis, characterization and non-linear optical response of organophilic carbon dots. Carbon 2013;61:640–9.
[27] Fowley C, McCaughan B, Devlin A, Yildiz I, Raymo FM, Callan JF. Highly luminescent biocompatible carbon quantum dots by encapsulation with an amphiphilic polymer. Chem Commun 2012;48(75):9361–3.
[28] Veronese FM, Pasut G. PEGylation, successful approach to drug delivery. Drug Discovery Today 2005;10(21):1451–8.

[29] Karakoti AS, Das S, Thevuthasan S, Seal S. PEGylated inorganic nanoparticles. Angew Chem Int Ed 2011;50(9):1980–94.
[30] Liu RL, Wu DQ, Liu SH, Koynov K, Knoll W, Li Q. An aqueous route to multicolour photoluminescent carbon dots using silica spheres as carriers. Angew Chem Int Ed 2009;48(25):4598–601.
[31] Mitra S, Chandra S, Pathan SH, Sikdar N, Pramanik P, Goswami A. Room temperature and solvothermal green synthesis of self passivated carbon quantum dots. RSC Adv 2013;3(10):3189–93.
[32] Hu SL, Niu KY, Sun J, Yang J, Zhao NQ, Du XW. One-step synthesis of fluorescent carbon nanoparticles by laser irradiation. J Mater Chem 2009;19(4):484–8.
[33] Zhu H, Wang X, Li Y, Wang Z, Yanga F, Yang X. Microwave synthesis of fluorescent carbon nanoparticles with electrochemiluminescence properties. Chem Commun 2009;34:5118–20.
[34] Jaiswal A, Ghosh SS, Chattopadhyay A. One step synthesis of C-dots by microwave mediated caramelization of poly(ethylene glycol). Chem Commun 2012;48(3):407–9.
[35] Wu D, Zhang F, Liang H, Feng X. Nanocomposites and macroscopic materials: assembly of chemically modified graphene sheets. Chem Soc Rev 2012;41(18):6160–77.
[36] Zhu S, Tang S, Zhang J, Yang B. Control the size and surface chemistry of graphene for the rising fluorescent materials. Chem Commun 2012;48(38):4527–39.
[37] Wang X, Cao L, Yang ST, Lu F, Meziani MJ, Tian L, et al. Bandgap-like strong fluorescence in functionalized carbon nanoparticles. Angew Chem Int Ed 2010;49(31):5310–4.
[38] Jia X, Li J, Wang E. One-pot green synthesis of optically pH-sensitive carbon dots with upconversion luminescence. Nanoscale 2012;4(18):5572–5.
[39] Zhu SJ, Zhang JH, Wang L, Song YB, Zhang GY, Wang HY, et al. A general route to make non-conjugated linear polymers luminescent. Chem Commun 2012;48(88):10889–91.
[40] Yang ZC, Li X, Wang J. Intrinsically fluorescent nitrogen-containing carbon nanoparticles synthesized by a hydrothermal process. Carbon 2011;49(15):5207–12.
[41] Helmchen F, Denk W. Deep tissue two-photon microscopy. Nat Methods 2005;2(12):2932–40.
[42] Liu Q, Guo B, Rao Z, Zhang B, Gong JR. Strong two-photon-induced fluorescence from photostable, biocompatible nitrogen-doped graphene quantum dots for cellular and deep-tissue imaging. Nano Lett 2013;13:2436–41.